academicJournals

Vol. 10(11), pp. 367-375, 15 June, 2015
DOI: 10.5897/SRE2015.6201
Article Number:2BFBED353458
ISSN 1992-2248
Copyright©2015
Author(s) retain the copyright of this article
http://www.academicjournals.org/SRE

Scientific Research and Essays

Full Length Research Paper

Analysis of cavitating flow through a venturi

Mohammed ZAMOUM* and Mohand KESSAL

Laboratoire Génie Physique des Hydrocarbures LGPH, Faculté des Hydrocarbures et de la Chimie FHC, Université M'hamed Bougara, Boumerdès, 35000, Algérie.

Received 1 March, 2015; Accepted 26 May, 2015

A dynamical study of a bubbly flows in a transversal varying section duct (Venturi), is modeled by the use of the mass and momentum phases equations, which are coupled with the Rayleigh-Plesset equation of the bubbles dynamics. The effects of the throat dimension and the upstream void fraction on flow parameters are investigated. The numerical resolution of the previous equations set let us found that the characteristics of the flow change dramatically with upstream void fraction. Two different flow regimes are obtained: a quasi-steady and a quasi-unsteady regimes. The former is characterized by a large spatial fluctuations downstream of the throat, which are induced by the pulsations of the cavitation bubbles. The quasi-unsteady regime corresponds to flashing flow in which occurs a bifurcation at the flow transition between these regimes. This transition occurs at $R_c \approx$ 4.3 which corresponds to $\alpha_s > 4.710^{-3}$. An analytical expression for the critical bubble size at the flashing flow point is also obtained and compared with theoretical data.

Key words: Venturi meter, tow-phase flow, cavitation.

INTRODUCTION

It is well known that the venturi is a robust technique for measuring the flow characteristics of a single-phase fluid for high Reynolds numbers. Multiphase flow measuring is generally more difficult. The density of a gas-liquid mixture depends upon the volume fraction of the gas, and the phases densities. The velocity of the gas within the venturi is likely to be different from that of the liquid. Over the two last decades, the investigations of a homogeneous steady-state cavitating nozzle flow, using spherical bubble dynamics with a polytropic thermal process (Wang and Brennen, 1998), have shown some flow instabilities illustrated by the flashing flow phenomenon.

The flow model, generally used, is a nonlinear continuum bubbly mixture which is coupled with the dynamics equation of the bubbles. A three equations model was first proposed by van Wijngaarden (1968, 1972), and has been used for studying steady and transient shock wave propagation in bubbly liquids, by omitting the acceleration of the mean flow. This model has been also considered by Wang and Brennen (1998), in the case of converging-diverging nozzle, with an upstream variable void fraction. It was observed that significant change of the flow characteristics depends strongly on the latter and a critical bubbles radius have been obtained. Considering the gas nucleation rate, as a

*Corresponding author. E-mail: m_zamoum2000@yahoo.fr, Tel: (00213)0552264618.
Author(s) agree that this article remain permanently open access under the terms of the Creative Commons Attribution License 4.0 International License

source term in the mass conservation equation of the bubbles, Delale et al. (2003) have used the previous model for the same converging-diverging nozzle. They have concluded that the encountered flow instability can be stabilised by thermal damping. Several authors have also considered the bubble dynamics equations under an appropriate form to the chosen example. Among them, Wang and Brennen (1999) have expressed the flow equations in time and radial coordinate, for a bubbly mixture, where the shock wave have been studied for spherical cloud of cavitating bubbles. Besides, effects of the shocks on the bubbles interactions have also been analysed. The same Rayleigh-Plesset equation has been used by Gaston et al. (2001) in modelling the bubbles as a potential source. The stream function has been written in function of spatial coordinates and the source term. They have analysed the effect of complex interactions through a venturi. By introducing liquid quantity and motion equation in a spatial Rayleigh-Plesset dynamics relation, Moholkar and Pandit (2001) have obtained a global dynamic equation which has been resolved in a three steps method. In their work they have studied the effect of the downstream pressure, the venturi pipe ratio, the initial bubble size and the upstream void fraction, on the dynamics of the flow. The results of the simulations show that the bubble/bubble and bubble/flow interaction through the hydrodynamic of the flow has important effect on the behaviour of the bubble flow. Considering a one bubble motion in a venturi, Soubiran and Sherwood (2000) have obtained a dynamic equation of the flow, based on different acting forces.

More recently, Ashrafizadeh and Ghassemi (2015) have experimentally and numerically investigate the effects of the geometrical parameters, such as throat diameter, throat length, and diffuser angle, on the mass flow rate, critical pressure ratio and application rang of small-sized cavitating venturis (CVs). The obtained results show that the CVs in very small size are also capable in controlling and regulating the mass flow rate while their characteristic curves are similar to those of ordinary CVs with larger throat sizes. Also, by decreasing the throat diameter of CVs, the choked mode region, the critical pressure and discharge coefficient decrease. By decreasing the diffuser angle from 15 to 5° in the numerical simulations, the critical pressure ratio increases and the discharge coefficient remains constant. By increasing the throat length of CVs, the critical pressure ratio decrease while discharge coefficient does not shown any changes. Also, a variable area cavitating venturi was designed and investigated experimentally by Tian et al (2014). Four sets of experiments were conducted to investigate the effect of the pintle stroke, the upstream pressure and downstream pressure as well as the dynamic motion of the pintle on the performance of the variable area cavitating venturi. The obtained results verify that the mass flow rate is independent of the downstream pressure when the downstream pressure ration is less about 0.8. The mass flow rate is linearly dependent on the pintle stroke and increases with the upstream pressure. The discharge coefficient is a function of the pintle stroke; however it is independent of the upstream pressure. They concluded that the variable area cavitating venturi can control and measure the mass flow rate dynamically.

Our investigation is based on the first model (a non linear continuum bubbly mixture model coupled with the dynamic equation of the bubble), the present work considers a cavitating flow through a venturi. The effect of the throat diameter of the venturi and the limits of flashing flow occurring for some upstream voids fraction, are analysed, and a critical value of bubble radius at the flashing flow point is obtained.

BASIC EQUATIONS

An axisymmetric venturi with cross-sectional area A(x) is showed in Figure 1, where the dimensions are reported to the inlet radius *a.* The liquid is assumed to be incompressible and the relative motion between the liquid and the duct wall is neglected and the total upstream bubble population is uniform without coalescence and further breaks up of the bubbles in the flow. Gas and vapor densities are neglected in comparison to one of the liquid. The bubbles are assumed to have the same initial radius R_S^*. Friction between the liquid and the duct wall is neglected and the relative motion between the tow phases ignored.
Then the mixture density can be expressed in function of bubble popula
tion

η: $\rho = \rho_L(1-\eta V)$

Where $V = 4/3\pi R^3(x,t)$ is the bubble volume.

Continuity and momentum equations of the bubbly flow (Wang and Brennen, 1998) are:

$$\frac{\partial}{\partial t}[(1-\alpha)A] + \frac{\partial}{\partial x}[(1-\alpha)uA] = 0 \quad (1)$$

$$\frac{\partial u}{\partial t} + u\frac{\partial u}{\partial x} = -\frac{1}{2(1-\alpha)}\frac{\partial Cp}{\partial x} \quad (2)$$

Where $\alpha(x,t) = 4/3\pi\eta R^3/\left[1+4/3\pi\eta R^3\right]$ is the bubble void fraction, and u(x, t) the fluid velocity.
$Cp(x,t) = \left(p^*(x,t) - p_s^*\right)/1/2\rho_L^* u_s^{*2}$ is the fluid pressure coefficient, and p(x, t) the fluid pressure, p_s^* the upstream fluid pressure, and u_s^* the upstream fluid velocity. The dynamics of the bubbles can be modeled by the Rayleigh-Plesset equation (Knapp et al., 1970; Daily and Hammitt, 1970; Plesset and Prosperetti, 1977).

$$R\frac{D^2R}{Dt^2} + \frac{3}{2}\left(\frac{DR}{Dt}\right)^2 + \frac{\sigma}{2}\left(1-R^{-3k}\right) + \frac{4}{Re}\frac{1}{R}\frac{DR}{Dt} + \frac{2}{We}\left(R^{-1}-R^{-3k}\right) + \frac{1}{2}Cp = 0 \quad (3)$$

Where $D/Dt = \partial/\partial t + u\partial/\partial x$ is the Lagrangian derivative,

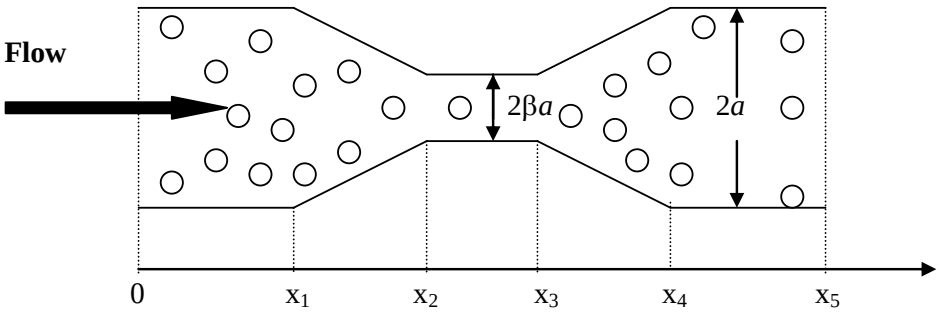

Figure 1. Schematic of the venture.

Table 1. Initial conditions and water characteristics .

Initial parameter	Water characteristics at 20°C
R_s^* =100 µm	ρ_L^* =1000 Kglm^3
u_s^* =10 m/s	μ_E^* =0.03 Ns/m^2
k=1.4	μ_L^* =0.001 Ns/m^2
Re=33	S*=0.073 N/m
σ=0.8	
We=137	

$\sigma = \left(p_s^* - p_v^*\right) / 1/2\rho_L^* u_s^2$ the cavitation number, p_v^* the partial pressure of vapor inside the bubble. $\mathrm{Re} = \rho_L^* u_s^* R_s^* / \mu_E^*$ is the Reynolds number, μ_E^* the effective viscosity of liquid. $\mathrm{We} = \rho_L^* u_s^{*2} R_s^* / S^*$ is the Weber number, S* represent the liquid surface tension, and ρ_L^* the liquid density.

Equations (1), (2) and (3) constitutes a simple model of one-dimensional two phase bubbly flow bubbly with a nonlinear bubble dynamics equation.

Steady-state solutions

Assuming steady-state conditions, all the partial time derivative terms in Equations (1) to (3) disappear. Then, Equation set (1) to (3) can be transformed into an ordinary differential equation set, with only one independent variable (x):

$$(1-\alpha)uA=(1-\alpha_s)=\text{constant} \tag{4}$$

$$u\frac{du}{dx} = -\frac{1}{2(1-\alpha)}\frac{dCp}{dx} \tag{5}$$

$$R\left(u^2\frac{d^2R}{dx^2} + u\frac{du}{dx}\frac{dR}{dx}\right) + \frac{3u^2}{2}\left(\frac{dR}{dx}\right)^2 + \frac{4}{Re}\frac{u}{R}\frac{dR}{dx} + \frac{2}{We}\left(\frac{1}{R} - \frac{1}{R^{3k}}\right) + \left(1 - \frac{1}{R^{3k}}\right) + \frac{1}{2}Cp = 0 \tag{6}$$

The corresponding initial conditions are:

$$R(x=0)=1, \quad U(x=0)=1, \quad Cp(x=0)=0 \tag{7}$$

The axial variation of the cross sectional takes the following from:

$$A(x) = \begin{cases} 1 & 0 < x < x_1 \\ 1 - \dfrac{(x - x_1)(1-\beta)}{x_2 - x_1} & x_1 < x < x_2 \\ \beta & x_2 < x < x_3 \\ 1 - \dfrac{(x_4 - x)(1-\beta)}{x_4 - x_3} & x_3 < x < x_4 \\ 1 & x_4 < x < x_5 \end{cases} \tag{8}$$

Where β is the dimensionless radius of the venturi throat, and x the distance along the axis. In the present work we assumed: β=0.5, x_1=3.0, x_2=5.7, x_3=6.7, x_4=10.5

RESULTS AND DISCUSSION

Equation set (4 to 6) is resolved by the use of a fourth order Runge-Kutta scheme, with some flow conditions (Table 1).

Venturi diameter throat effect

Three non-dimensional diameters ventuti throat (β) 0.5, 0.6 and 0.7 were tested numerically. Effect of the bubble radius evolution is showed in Figure 3 for some non-

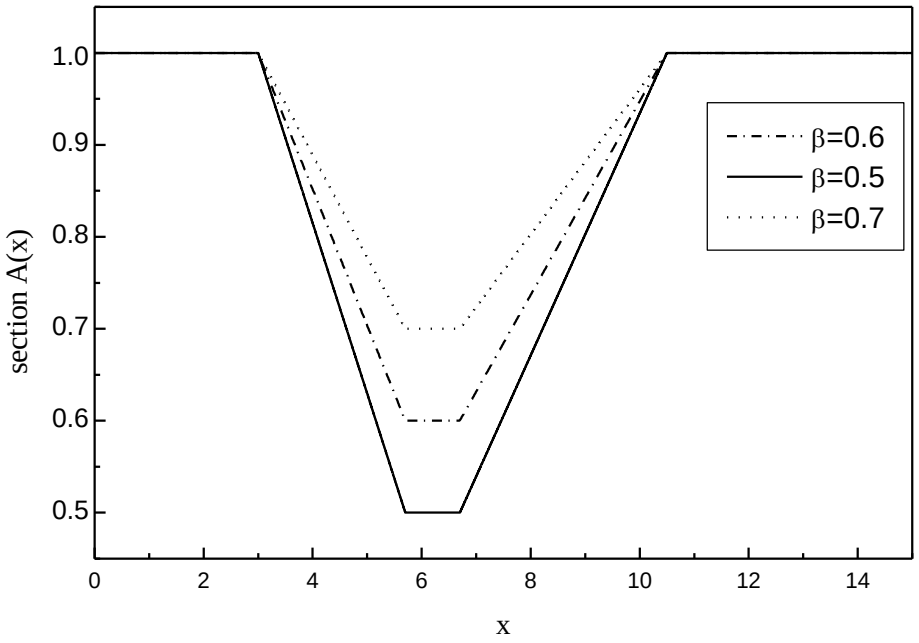

Figure 2. Venturi sections for various values of the non-dimensional throat radius β.

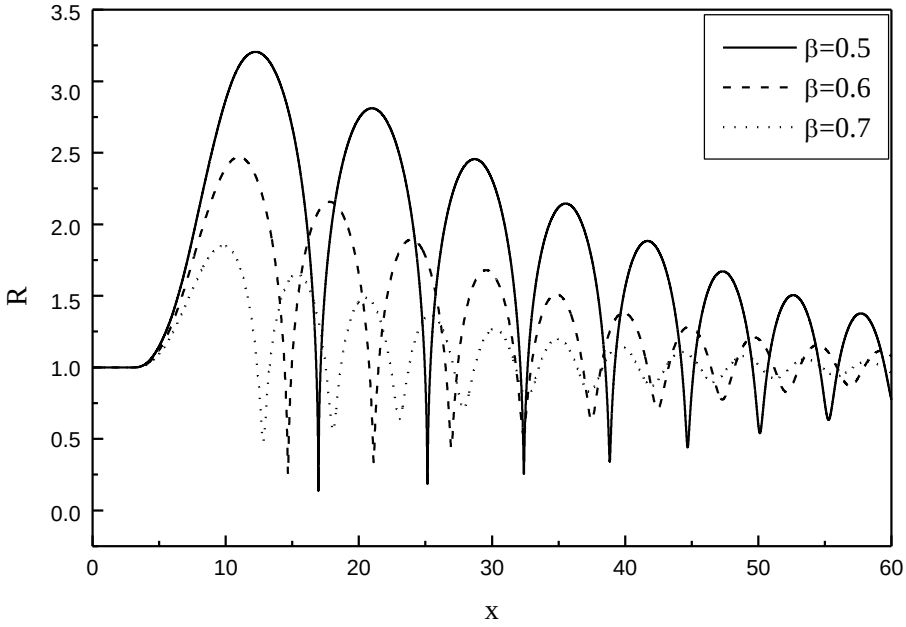

Figure 3. Bubbles radius for various values of the non-dimensional throat radius β.

dimensional diameters of the venturi throat (Figure 2). By increasing the diameters venturi throat, the bubble radius decrease and the bubble oscillations frequency increase. Fluid axial velocity and pressure distribution are drawn in Figures 4 and 5, for different throat diameters. It seems that the evolution of these parameters corresponds to the monophasic case (Figure 4). In the Figure 6, the axial bubble radius gradient gives a large value after the throat section which is due to the inertial phenomena, as explained in Blak (1949) work. A strongly dumping is also observed for the subsequent peaks. Figure 7, shows a part of the previous (Figure 6), corresponding to a small distance, where the continuity of radius gradient can be verified.

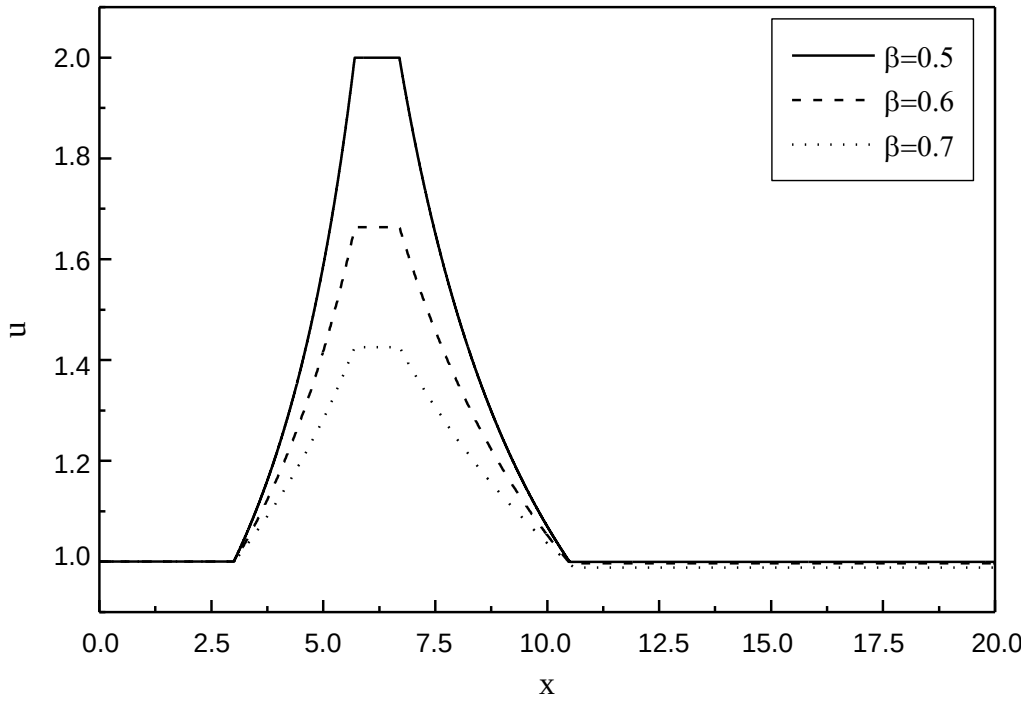

Figure 4. Fluid velocity for various values of the non-dimensional throat radius β.

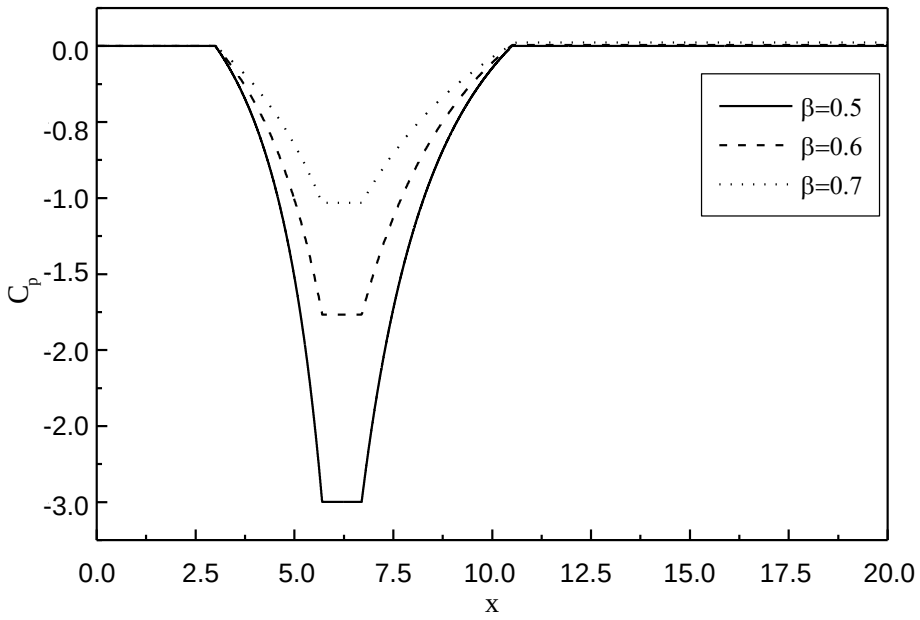

Figure 5. Fluid pressure for various values of the non-dimensional throat radius β.

Upstream void fraction effect

Five different upstream void fractions (α_s) of the order of 10^{-3} are used in the computation to study, the effect of the upstream void fraction on the flow structure through the ventuti. The case of α_s=0 corresponds to the incompressible pure liquid flow, the results are shown in Figures 8, 9 and 10 which correspond to the non-dimensional bubble radius distribution, fluid velocity and fluid pressure coefficient, respectively, an instability

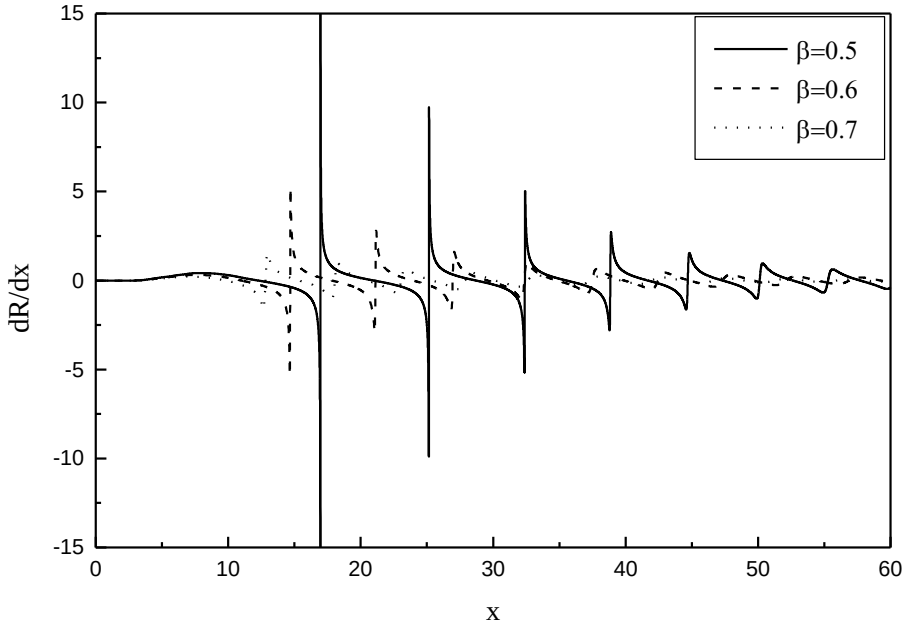

Figure 6. Bubble radius gradient for various values of the non-dimensional throat radius β.

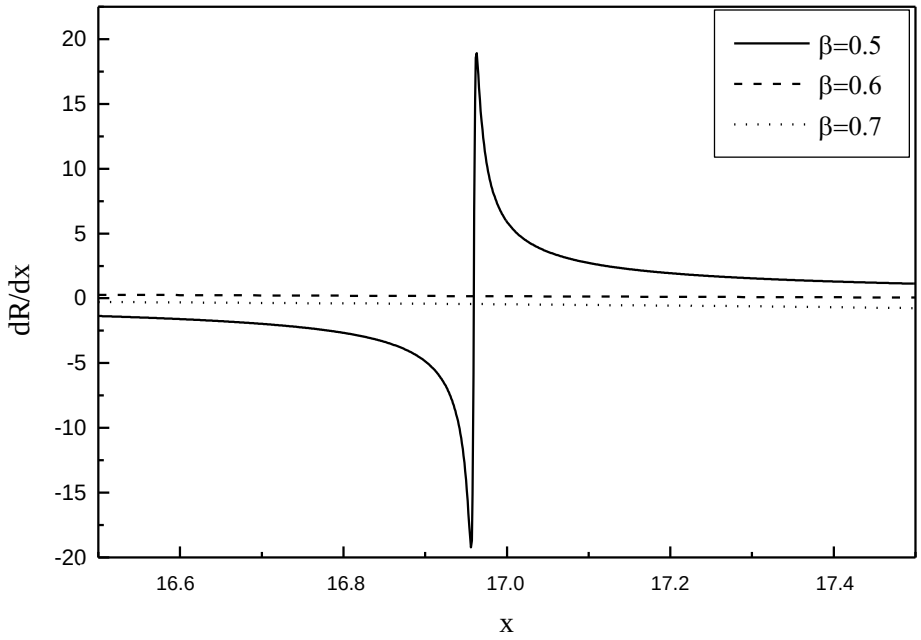

Figure 7. A part of Figure 6.

inception can be remarked in these figures, which is located just after the throat, these results confirm those of Wang and Brennen (1998) with no important differences.

Figure 8 shown that the bubble size reach the maximum after passing the nozzle throat of the venturi with increase in the upstream void fraction, the maximum size of the bubbles increases and bubble frequency oscillation decrease, this maximum size is shifted further downstream after it reach the critical radius (instability occurs), the bubbles growth without bound in the calculation, this instability occurs when the bubble reaches a critical value, also the void fraction growing

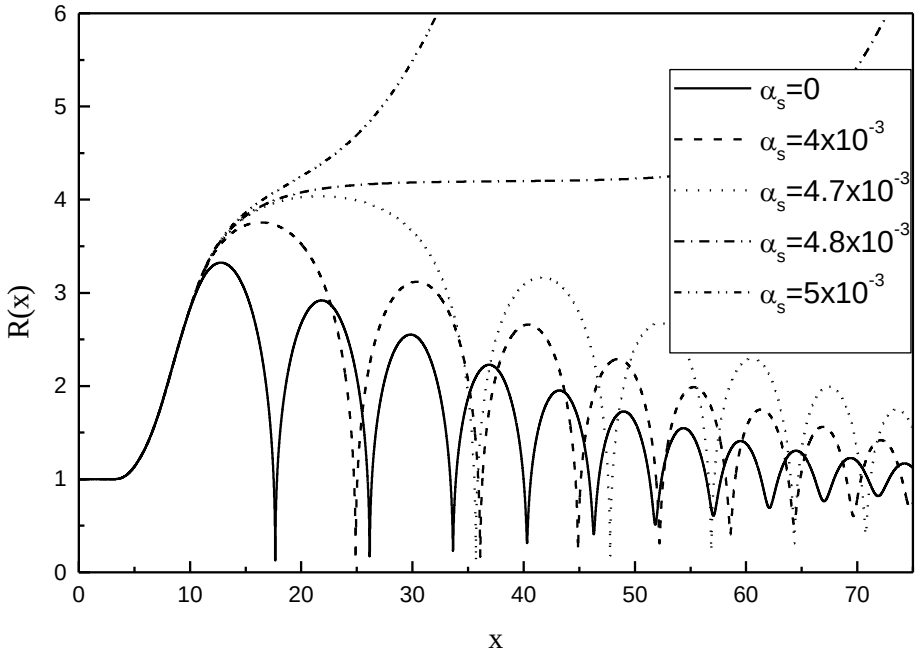

Figure 8. Axial bubble radius distribution for deferent upstream void fraction.

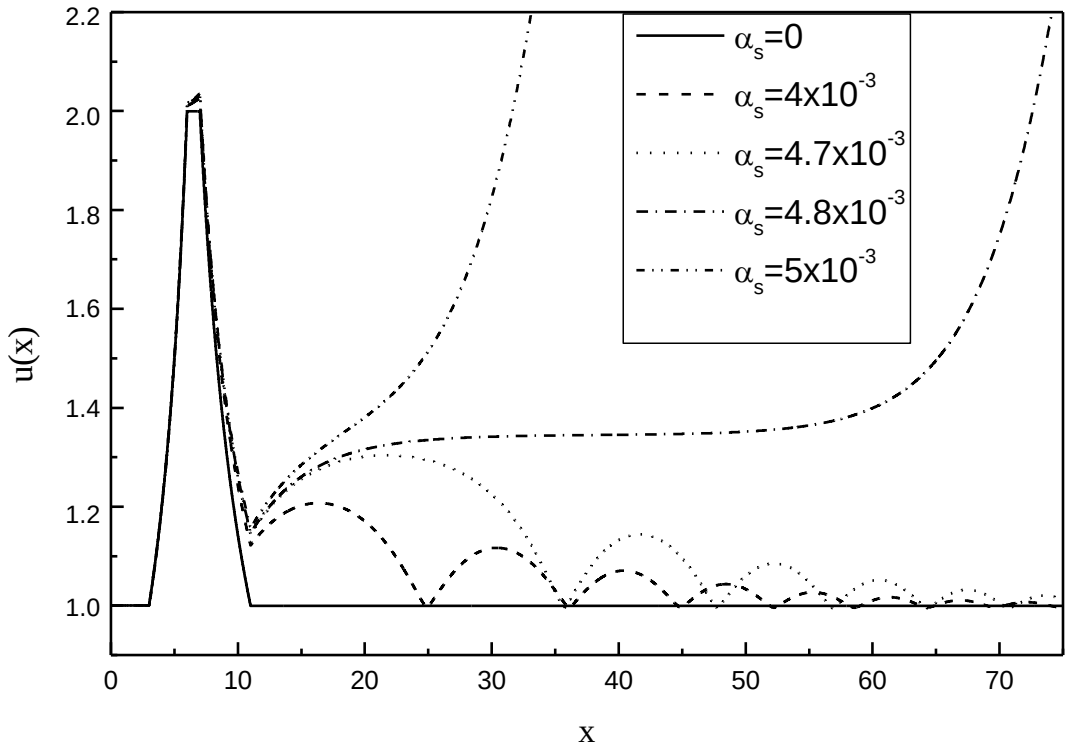

Figure 9. Axial fluid velocity distribution for different upstream void fractions.

leads to large amplitudes of the previously drown parameters, an important remark concerns the venturi geometry effect: in the Wang and Brennen (1998) work, where cavitation in converging-diverging nozzle bubbly

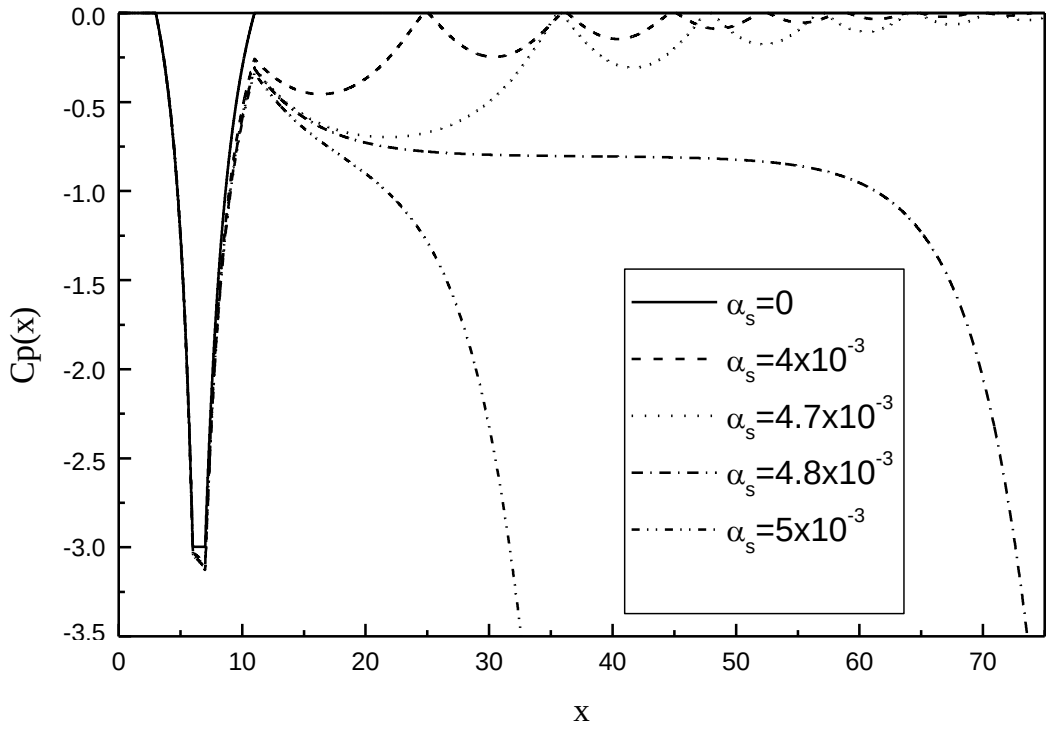

Figure 10. Fluid pressure coefficient for different upstream void fraction.

flow is studied. It can be observed that instability occurs for an upstream void fraction α_s>3,045.10^{-6}, which corresponds to a critical bubble radius r_c≈51. whereas, for our geometry (Figure 1), the same phenomenon occurs for α_s> 4,7.10^{-3}, with r_c≈4,3. This difference is due to the throat nozzle geometry. An other difference between these geometry's concerns the numerical implementation in the first case (Wang and Brennen, 1998) a variable space step is required, contrarily to the second case where a constant and relatively large space step is sufficient in the practice r_c correspond the flashing flow inception, which is illustrated by an instability of the parameters flow analytical expression for r_c is obtained by Wang and Brennen (1998), $R_c \approx (\sigma / 2\alpha_c)^{1/3}$, where α_c is the upstream void fraction at which flashing flow occurs.

The fluid velocity is illustrates in Figure 9. The presence of the bubble in the upstream flow results in the downstream fluctuations of the flow. With increase the upstream void fraction, the amplitude of this velocity fluctuations downstream increase and its frequency oscillation decrease. However, as a, increases to a critical value of the upstream void fraction, the flashing flow occurs, the velocity increases dramatically and the flow becomes unstable. Due to the Bernoulli effects, the fluid pressure coefficient varies inversely with the fluid velocity (Figure 10). Figure 11 illustrates the Bubble radius gradient in the flow for different upstream void fraction. Due to the inertial phenomena, the bubble radius gradient becomes a large value after the throat section of the venturi and a strongly dumping is also observed for the subsequent peaks. These peaks are reduced and amortized far further downstream flow.

CONCLUSION

A steady state equation set is considered for a bubbly two phase flow across a venturi. We have shown the effect of throat diameter and upstream void fraction on the characteristics parameters flow evolution. In the obtained result, we found that the upstream void fraction strongly affect the structure of the flow. Two different flow regimes are obtained: quasi-steady and quasi-unsteady regimes, where the transition between them is illustrated by a flashing flow inception. The latter phenomenon occurs at R_c≈ 4.3 which corresponds to α_s> 4.710^{-3}. This value is compared with the case of converging-diverging nozzle which indicates that the converging-diverging nozzle presents more stability than the venturi. This analytical result is numerically tested for a venturi. Also we have shown the inflexion point position and the corresponding bubble radius and void fraction.

Conflict of Interest

The authors have not declared any conflict of interest.

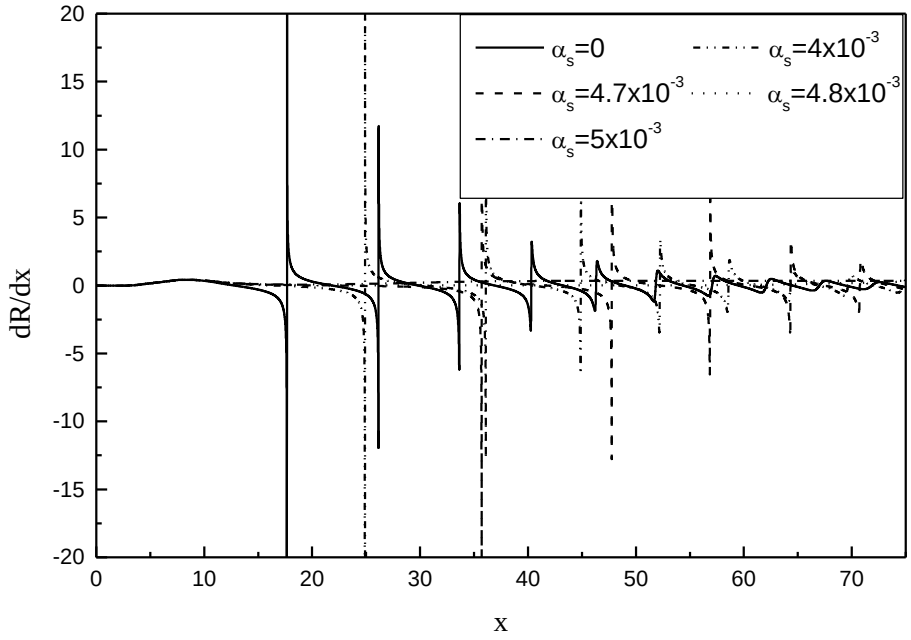

Figure 11. Bubble radius gradient for different upstream void fraction.

Nomenclature

A: dimensionless cross-sectional area of the Venturi, A^*/A_s^*, A*: cross-sectional area of the Venturi, A_s^*: upstream cross-sectional area of the Venturi, Cp: fluid pressure coefficient, $\left(p^* - p_s^*\right)/1/2\rho_L^* u_s^{*2}$, R: dimensionless bubble radius, R^*/R_s^*, R_c: dimensionless critical bubble radius at which flashing flow occurs, R_s^*: upstream bubble radius, Re: Reynolds number, $\rho_L^* u_s^* R_s^*/\mu_E^*$, S*: surface tension of the liquid, We: Weber number, $\rho_L^* u_s^{*2} R_s^*/S^*$, k: polytropic index for the gas inside the bubbles, p^*: fluid pressure, p_s^*:upstream pressure, p_v^*: vapor pressure, T: dimensionless time, $t^* u_s^*/R_s^*$, t*: time, u: dimensionless fluid velocity, u^*/u_s^*, u*: fluid velocity, u_s^*: upstream fluid velocity, V: volume of the bubble, $V = 4/3\pi R^3$, x: dimensionless Eulerian coordinate, x^*/R_s^*, x*: Eulerian coordinate.

Greek Letters

α: void fraction of the bubbly fluid, α_c: upstream void fraction at which flashing occurs, α_s: upstream void fraction, β: dimensionless radius of the Venturi throat, η: dimensionless bubble population per unit liquid volume, $\eta^* R_s^{*3}$, η^*: bubble population per unit liquid volume, γ: ratio of specific heats of the gas inside the bubbles, μ_E^*: effective dynamic viscosity of the liquid, ρ:dimensionless fluid density, ρ_L^*: density of the liquid, σ: cavitation number, $\left(p_s^* - p_v^*\right)/1/2\rho_L^* u_s^{*2}$.

REFERENCES

Ashrafizadeh SM, Ghassemi H (2015). Experimental and numerical investigation on the performance of small-sized cavitating venturis. Flow measurement and Instrumentation, 42:6-15.

Blak FG (1949). The tensile strength of liquids. A review of the literature. Harvard coustics Res. Lab. TM 9, June.

Delale CF, Okita K, Matsumoto Y (2003). Steady-State cavitating nozzle flows with nucleation. Fifth international symposium on cavitation. Osaka, Japan, November 1-4.

Gaston MJ, Reizes JA, Evans GM (2001). Modelling of bubble dynamics in a Venturi flow with a potential flow method. Chem. Eng. Sci. 65:6427-6435.

Knapp RT, Daily JW, Hammitt FG (1970). Cavitation. New York: Me Graw Hill.

Moholkar VS, Pandit AB (2001). Numerical investigations in the behaviour of one-dimensional bubbly flow in hydrodynamic cavitation. Chem. Eng Sci. 56:1411-1418.

Plesset MS, Prosoeretti A (1977). Bubble dynamics and cavitation. Annual review of fluid mechanics, 9:145-185.

Soubiran J, Sherwood JD (2000). Bubble motion in a potential flow within a Venturi. J. Multiphase Flow. 26:1771-1796.

Tian H, Zeng P, Yu N, Cai G (2014). Application of variable area cavitating venturi as a dynamic flow controller. Flow Measurement and Instrumentation.38:21-26.

van Wijngaarden L (1968). On the equations of motion for mixtures of liquid and gas bubbles. J. Fluid Mech. 33:465-474.

van Wijngaarden L (1972). One-dimensional flow of liquids containing small gas bubbles. Annual Rev. Fluid Mech. 4:369-396.

Wang YC, Brennen CE (1998). One-dimensional bubbly cavitating flows through a converging-diverging nozzle. J. Fluids Eng. 120:166-170.

Wang YC, Brennen CE (1999). Numerical computation of shock waves in a spherical bubble cloud of cavitation bubbles. J. Fluids Eng. 121:872-880.